Gas-Phase Reactions of U^+ and U^{2+} with O_2 and H_2O in a Quadrupole Ion Trap

Glen P. Jackson,[†,‡] Fred L. King,[†] Douglas E. Goeringer,[‡] and Douglas C. Duckworth*[,‡]

Department of Chemistry, West Virginia University, Morgantown, West Virginia 26506-6045, and Chemical Sciences Division, P.O. Box 2008, Oak Ridge National Laboratory, Oak Ridge, Tennessee 37831-6375

Received: April 15, 2002; In Final Form: June 20, 2002

Reaction pathways and rate constants of gas-phase uranium and uranium oxide ions with O_2 and H_2O have been investigated using a quadrupole ion trap mass spectrometer (QIT-MS). A new reaction pathway is identified for the reaction between U^{2+} and H_2O, which leads to the formation of UO^+ via the intermediate UOH^{2+}. Reaction rate constants are determined for several reactions by measuring the reaction rate at different partial pressures of the reagent gas and are found to be in reasonable agreement with the literature. These rate constants include the first known measurement for the reaction of U^{2+} with H_2O ($\sim$0.4 k_{ADO}). New limits on thermochemical values are also provided for certain species. These include ΔH_f (UO^{2+}) $\leq$ 1742 kJ mol^{-1} and 1614 $\leq \Delta H_f$ (UOH^{2+}) $\leq$ 1818 kJ mol^{-1} and are based on the assumption that only exothermic or thermoneutral reactions are possible under the conditions used. This assumption is supported by simulations of the root-mean-square (RMS) ion kinetic energy of stored uranium ions in the QIT. Only a slight increase in the RMS ion kinetic energies, from 0.1 to 0.2 eV, is predicted over the range of trapping conditions studied ($0.05 \leq q_z \leq 0.75$) corresponding to a theoretical reaction temperature of $\sim$384 K. The simulations also compare helium and neon as bath gases and show that the RMS kinetic energies are found to be very similar at long trapping times (>20 ms), although neon establishes steady state conditions in approximately half the time.

1. Introduction

Quadrupole ion traps (QITs) serve as one of the most versatile mass spectrometers available to physicists, chemists, and biochemists. It is possible to store ions of either charge, or both charges simultaneously, up to several kilodaltons in mass.[1] Trapped ions can be dissociated by a variety of methods in order to obtain thermodynamic or structural information.[2] It is also possible to study ion molecule reactions by substituting part or all of the bath gas with a reagent gas of interest.[3] Furthermore, by introducing a known quantity of reagent, and allowing a reaction to occur for a known time period, it is possible to determine the rate constant for an ion−molecule reaction.[3] Bonner et al. were the first to demonstrate the possibility of measuring rate constants in the QIT by studying the charge and proton-transfer reactions between small organic molecules.[4] Such determinations are often dependent on temperature.[5] To obtain meaningful quantitative data it is important to ascertain the temperature or kinetic energy of the colliding partners.[6] In ion beam experiments, the acceleration voltage leading to the reaction chamber determines the kinetic energy. In ion traps, however, quantification of the kinetic energy of the ions is somewhat more complicated, especially when a bath gas is introduced into the trapping region to dampen the kinetic energy of the ions.

Numerous investigators have reported reaction rate constants of gas-phase ion−molecule reactions and the mean kinetic energies associated with trapped ions.[4,7−17] These reactions were conducted almost exclusively in helium. The general conclusions are that the kinetic energy of trapped ions increases as a function of increasing trapping potential and decreasing bath gas pressure. An increase in kinetic energy can either increase or decrease the rate of a reaction depending on the thermodynamics involved. Rates of exothermic reactions often decrease with increasing kinetic energy, whereas the rates of endothermic reactions tend to increase with increasing kinetic energy.

The presence of a bath gas to buffer the ion kinetic energy is useful for reducing the influence of the trapping potential. Helium is the most commonly used bath gas, at pressures of $\sim(0.1-1) \times 10^{-3}$ Torr. At this time, no direct comparisons of different bath gases have been published to determine how the gases might affect the kinetic energy or internal energy of the ions in the QIT. It has been shown, however, that increasing the partial pressure of N_2 in a constant trap pressure of 1.7 mTorr He/N_2 can increase the internal energy of a molecular ion.[16] It is not known to what extent this observation is related to the center of mass collision energy or collision frequency, etc. This manuscript will present simulations in order to predict the effect of using a bath gas heavier than helium.

Recent studies in our laboratory measured the kinetics of collision induced dissociation (CID) of strongly bound metal oxides (D_0 > 800 kJ mol^{-1}) in QITs.[18−20] To dissociate these strongly bound oxides, experiments were performed with neon (in place of helium) in order to achieve the high internal temperatures required. The metal oxides studied were formed via metal ion reactions with O_2 in the trap. Because very few studies have considered the effect of a heavier bath gas on reaction rates, it was questioned how well the oxidation rates could be measured in the QIT using neon as the bath gas. The reaction rates of uranium ions with O_2 are measured here and compared with literature values to assess the accuracy of this method. The approach is also used to probe other reaction rates.

* Corresponding Author. E-mail: duckworthdc@ornl.gov. Phone: (865) 576 6296. Fax: (865) 574-6906.
† West Virginia University.
‡ Oak Ridge National Laboratory.

10.1021/jp0259420 CCC: $22.00
Published on Web 08/02/2002

Ion isolation and double resonance ejection experiments are also used to probe reaction pathways and thermodynamics of uranium ions with oxygen and water. The ability to detect and eject ions, selectively, at 0.5 *m/z* resolution reveals a previously unknown gas-phase oxidation pathway for the doubly charged uranium ion with water.

2. Experimental Apparatus and Method of Measurement

The pulsed glow discharge ion trap mass spectrometer used in this study has been described in detail elsewhere.[21] A uranium pin of natural isotopic abundance served as the sample cathode and was positioned on a direct insertion probe.[22] Neon was used as the glow discharge support gas at a pressure of 0.8 Torr and as the ion trap bath gas at 0.5 mTorr. A leak valve (Series 203, Granville-Phillips, Boulder, CO) introduced compressed oxygen (Air Liquide) or water (vapor) at pressures between 9×10^{-7} and 7×10^{-6} Torr. Isotopically enriched $H_2{}^{18}O$ (66 atom % ^{18}O, Isotec Inc., Miamisburg, OH) was used to verify the source of oxygen in the reactions involving water. An ion gauge (Vacuum Instrument Corporation, Ronkonkoma, NY) measured the pressure of oxygen (or water) before the addition of the neon bath gas and after each experiment when the neon had been evacuated.

The reaction time for the isolated ion of interest and the reagent molecule is defined as the time between the last isolation event in the scan function and the initiation of the mass spectrum. In reality, ions will continue to react during the scan function until such time as they are ejected and detected. But because the reagent ions are always the lightest (in these experiments) and the first to be ejected in the scan function (after <2 ms), no correction is necessary in these experiments to account for the reactions occurring during the acquisition period. An automated "experiment editor" varied the reaction period so that in a typical experiment, 16 mass spectra were averaged to obtain intensity measurements at 2 ms intervals from 0 to 50 ms reaction time. Plots of the reactant ion signal intensity versus time were thereby generated. The rates were verified to be pseudo-first order so that the temporal plots could be converted to a phenomenological rate, *nk*, according to the expression

$$-\ln\left(\frac{[M^+]_t}{[M^+]_0}\right) = nkt \qquad (1)$$

where n is the number density of the reagent gas, $[M^+]_0$ is the initial ion signal of reagent ion, and $[M^+]_t$ is the reagent ion signal at time t. This equation also assumes a linear relationship between ion signal, as measured by the ion detector, and the number of ions (a valid assumption over small ranges).

By repeating the experiment at various values of n (different reagent gas pressures) the pseudo-first-order rate constant k can be obtained from the slope of the plot *nk* versus n. If the rate constant for a given reaction is known, the measured rates could be used to calibrate the ion gauge.[7] The fitted slopes of *nk* versus n are not forced through zero because reactions are observed to occur when no reagent gases are added (i.e., n is actually a sum of $n_{residual}$ and n_{added}, where $n_{residual}$ is the residual number density of O_2 arising from contaminants in the vacuum system). Quantification of the initial reagent concentration, $n_{residual}$, is possible, by determining the x-intercept of the slopes in Figures 4 and 5. In this study, a complication in the determination of $n_{residual}$ for O_2 is that trace levels of H_2O are also present (in larger abundance) and contribute to the oxidation reactions of uranium ions. In these experiments, we assume that the residual pressures of O_2 and H_2O remain constant throughout, and therefore do not affect the determination of the rate constants from the slopes. This assumption is supported by the correlation of the least squares curve fitting.

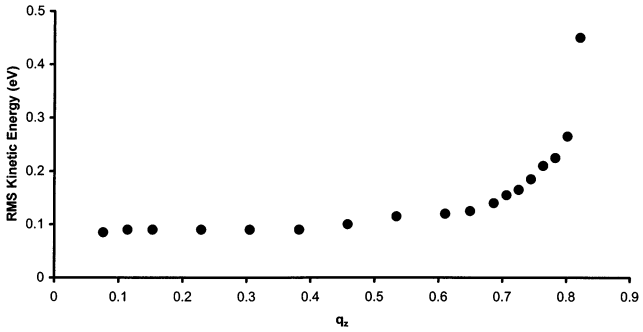

Figure 1. Simulated root-mean-square (RMS) ion kinetic energy of uranium ions as a function of Mathieu parameter q_z (1 mTorr Ne).

3. Results and Discussion

3.1. Kinetic Energy Considerations. According to previous reports, the mean kinetic energy of an ion in the ion trap will be approximately 0.1−2 eV following 15 collisions in $\sim(1-5) \times 10^{-3}$ Torr He.[12−14] When a bath gas is present, the kinetic energy of the ions increases only slightly with increasing trapping potential until a stability boundary is approached. Because most experiments are performed in helium, very little is reported about the effects of using a heavier bath gas such as neon. To obtain a better understanding of the kinetics of ions trapped in a neon bath gas at different trapping potentials, calculations were performed using ITSIM software.[23] For comparison, calculations were performed with both helium and neon as bath gases. The simulation modeled 500 ^{238}U ions at a pressure of 1 mTorr bath gas at 300 K. In Figure 1, the root-mean-square (RMS) kinetic energy of U^+ in neon is plotted as a function of q_z to show that once steady-state conditions are established there is very little difference in RMS kinetic energy between $0.1 \leq q_z \leq 0.65$. At steady state, no significant difference is found between helium and neon as bath gases (data not shown). At a q_z of 0.67, at which the presented experiments are conducted, the calculated RMS kinetic energy is $\sim$0.13 eV.

The total kinetic energy, KE_{total}, of ions moving through a buffer gas under the influence of an electric field is comprised of terms related to motion in the direction of the field and stochastic motion due to ion-buffer gas collisions. The relative (center-of-mass) kinetic energy between the ions and buffer gas is[24] $KE_{stochastic} = 3/2k_B T^k_{eff}$, where

$$T^k_{eff} = T_{buf} + \frac{m_{buf}}{3k_B} v^2_{directed} \qquad (2)$$

and T^k_{eff} is the ion effective translational temperature associated with $KE_{stochastic}$, T_{buf} is the buffer gas temperature, $v_{directed}$ is the ion velocity in the direction of the field, m_{buf} is the mass of the buffer gas, and k_B is the Boltzmann constant. Furthermore, the relative (center-of-mass) kinetic energy between the ions and neutral reactants, $KE^{rxn}_{stochastic} = 3/2k_B T^{rxn}_{eff}$, is given by[24]

$$T^{rxn}_{eff} = T_{buf} + \frac{m_r}{3k_B} v^2_{directed}\left(\frac{m_{ion} + m_{buf}}{m_{ion} + m_r}\right) \qquad (3)$$

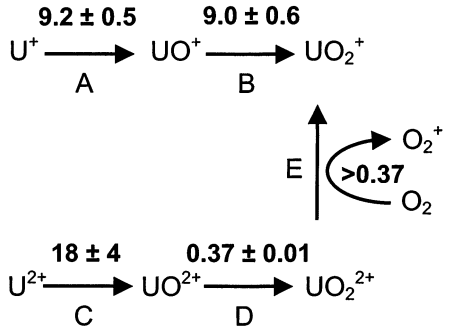

Figure 2. Measured reaction rates and pathway for the reactions of U^{2+} and U^+ with O_2. Rates shown have units 10^{-10} cm^3 s^{-1}.

where $T_{\text{eff}}^{\text{rxn}}$ is the effective translational temperature for the reaction rate coefficients, and m_{ion} and m_{r} are the ion and reactant masses, respectively. A good estimate of v_{directed} can be obtained from the Wannier equation[25] for the total laboratory kinetic energy, KE_{lab}.

$$\text{KE}_{\text{lab}} = 3/2k_{\text{B}}T_{\text{buf}} + 1/2m_{\text{ion}}v^2_{\text{directed}} + 1/2m_{\text{buf}}v^2_{\text{directed}} \quad (4)$$

The first term on the right-hand side is due to the thermal energy of the buffer gas, the second term results from the velocity of the ion packet, and the last term is due to conversion of ion drift motion to random motion via collisions with the buffer gas.

Because ions generally were stored at low trapping potentials for at least 20−25 ms before the reaction period, they are assumed to be kinetically cooled to approximately the calculated RMS kinetic energy. For the reaction, $U^+ + O_2$, making the approximation $\text{KE}_{\text{total}} \approx 0.13$ eV, solving eq 4 for v_{directed}, and substituting into eq 3 yields $T_{\text{eff}}^{\text{rxn}} \approx 384$ K; the corresponding relative kinetic energy of the reactants $\text{KE}_{\text{stochastic}}^{\text{rxn}} \approx 0.050$ eV (4.8 kJ mol^{-1}). The maximum internal energy of the neutral reactant is equal to $\text{KE}_{\text{stochastic}}^{\text{rxn}}$ (only electronic excitations are possible for atomic ions), thus implying that the observed reactions are unlikely to be endothermic by more than ~5 kJ mol^{-1}, which is well within the error of most reported enthalpies. For the case of diatomic ions under similar reaction conditions, the maximum internal energy (now partitioned between ions and neutral reactants) is also $\text{KE}_{\text{stochastic}}^{\text{rxn}}$ and therefore does not contribute significantly to the energy available for activation/reaction. In all the reactions considered here, two moles of reagents react to form two moles of products, so entropy effects are negligibly small (at near-room-temperature conditions) and are therefore ignored.

3.2. Reactions with O_2. Figure 2 summarizes the reaction pathways examined in this study that involve molecular oxygen. Shown next to each arrow is the measured rate constant ($\times 10^{-10}$ cm^3 s^{-1}). The rate constants for reactions of singly charged uranium ions with oxygen have been known for some time,[26] but reaction rate constants for the doubly charged species have been measured only recently.[27] Tables 1−3 provide thermodynamic and kinetic data both from literature and from results derived in this work. Enthalpies of formation in Table 1 (with the exception of UO^{2+} and UOH^{2+}) were used to calculate the enthalpies of reactions in Tables 2 and 3. For UO^{2+} and UOH^{2+}, limits for the enthalpies of formation were determined from the exothermic reactions observed and reported in Tables 2 and 3. Other values necessary for the calculations (e.g., $\Delta H_{\text{f}}(\text{O})$, $\Delta H_{\text{f}}(\text{H}_2\text{O})$) are taken from reference 28, with the exception of the gas-phase proton affinity of water that is taken from reference 29.

TABLE 1: Thermochemical Data of Species of Interest

species (M)	ΔH_{f} M$_{(\text{g})}$ (kJ mol^{-1})
U^{2+}	2277 ± 50[35]
UO^{2+}	<2047[33]
	<1747[a]
UOH^{2+}	1410−1818[a]
UO_2^{2+}	1553 ± 250[33]
U^+	1129 ± 4[28,35]
UO^+	582[35]
UOH^+	516 ± 35[34]
UO_2^+	54 ± 50[35]
	57[28,35]
	88 ± 20[34]
O•	249 ± 0.1[28]

[a] This work.

TABLE 2: Reactions of Singly Charged Uranium Species with Molecular Oxygen and Water

reactants	products	ΔH_{r} (kJ mol^{-1})	rate constant ($\times 10^{-10}$ cm^3 s^{-1})
$U^+ + H_2O$	$UO^+ + H_2$	−289	8.1[a]
		±30[34]	11 ±2[c]
$U^+ + H_2O$	$UOH^+ + H$	≤0[34]	see text
$U^+ + O_2$	$UO^+ + O$	−280	6.5[a]
		±30[34]	8.6[b]
			5.6[34]
			8.5 (−1 +4)[26]
			9.2 ± 0.5[c]
$UO^+ + H_2O$	$UO_2^+ + H_2$	−260	0.69[a]
		±37[34]	0.15 ± 0.05[c]
$UO^+ + O_2$	$UO_2^+ + O$	−255	5.26[a]
		±37[34]	10[b]
			9.0 ± 0.6[c]

[a] Calculated from ref 30 using k_{ADO} theory[32] and values from ref 28. [b] Calculated from decay constants in ref 27 assuming 20% partial pressure of O_2 in air at 4×10^{-5} Torr air pressure. [c] This work.

TABLE 3: Reactions of Doubly Charged Uranium Species with Molecular Oxygen and Water

reactants	products	ΔH_{r} (kJ mol^{-1})	rate constant ($\times 10^{-10}$ cm^3 s^{-1})
$U^{2+} + H_2O$	$UO^{2+} + H_2$	<11[a]	10[d]
		≤ 0[d]	
$U^{2+} + H_2O$	$UOH^{2+} + H$	≤ 0[d]	see text
$U^{2+} + O_2$	$UO^{2+} + O$	≤0[27,33,d]	11[c]
			13[b]
			18 ± 4[d]
$UO^{2+} + H_2O$	$UO_2^{2+} + H_2$	not observed	<0.1[d]
$UO^{2+} + H_2O$	$UO^{2+} + H_2O^+$	not observed	<0.1[d]
$UO^{2+} + O_2$	$UO_2^+ + O$	≤0[27,33,d]	0.44[c]
			0.3[b]
			0.37 ± 0.1[d]
$UO^{2+} + O_2$	$UO^+ + O_2^+$	>0[c,27,33]	$<0.37 \pm 0.1$[d]
$UOH^{2+} + H_2O$	$UO^+ + H_3O^+$	≤ 0[d]	
$UOH^{2+} + H_2O$	$UOH^+ + H_2O^+$	−84[a]	
$UO_2^{2+} + O_2$	$UO_2^+ + O_2^+$	≤0[27,33,d]	6.2[b]
			3.8[c]

[a] Calculated. [b] Calculated from decay constants in ref 27 assuming 20% partial pressure of O_2 in air at 4×10^{-5} Torr air pressure. [c] Calculated from ref 33 assuming collision rates for U^{2+}, UO^{2+}, UO_2^{2+} with O_2 to be $\sim 1.1 \times 10^{-11}$ (see the end of section 3.2.1 for details). [d] This work.

3.2.1. U^+ Reaction with O_2. The thermodynamic and kinetic aspects of reaction A are well known, and this reaction provides a suitable probe system for the ion trap.

$$U^+ + O_2 \rightarrow UO^+ + O \quad (A)$$

Experiments were first conducted to ensure that charge conservation is maintained and that the reaction from U^+ to UO_2^+

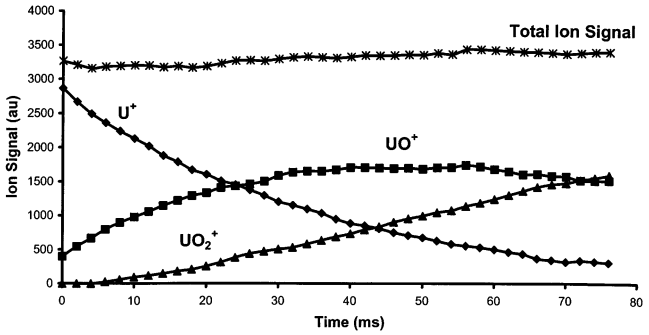

Figure 3. Ion signal intensities versus time for the reaction of U^+ with O_2 (1.3×10^{-6} Torr O_2). Bath gas is neon at 0.5 mTorr, $q_z = 0.6$.

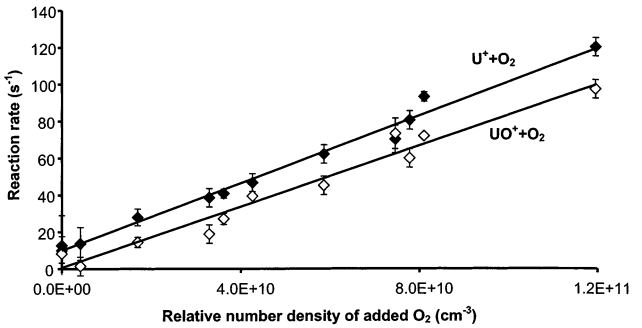

Figure 4. Measured reaction rates of U^+ (filled diamonds) and UO^+ (open diamonds) with O_2 versus relative number density of added O_2. Values shown are the average of four different q_z values on three separate days with ±1 s.d.

does in fact proceed through the intermediate UO^+. Figure 3 is a plot of the ion signal intensities of each species as a function of time for the reaction $U^+ + O_2$ at a nominal oxygen number density of 4×10^{10} cm^{-3}($\sim 1.3 \times 10^{-6}$ Torr). The constant total ion signal demonstrates that charge conservation is maintained. The temporal profiles shown in Figure 3 are indicative of a two-step reaction sequence in which the reaction proceeds through the intermediate UO^+.[30] Resonance ejection of the intermediate UO^+ confirmed that all the U^+ losses were accounted for in the UO^+ channel. Therefore, the measured decrease in ion signal of U^+ over time can be used to calculate the rate of reaction A according to eq 1.

Reaction rates for reaction A were measured at four different trapping potentials between $0.2 \leq q_z \leq 0.8$ at four different pressures of O_2. The trapping potential had no statistically significant affect on the measured reaction rates for this reaction, based on the external precision of the measurements. This observation is consistent with the simulations presented earlier, whereby the RMS kinetic energy of uranium ions did not significantly increase over this range of trapping potentials. Although this specific reaction is not highly sensitive to kinetic energy effects, the reaction rates have been shown to decrease (~10%) as the kinetic energy of the U^+ increases (from 0 to 5 eV in lab frame).[26] A reaction that is more sensitive to kinetic effects would be required to examine further the effects of rf heating at different values of q_z.

The reaction rates for U^+ at several trapping potentials were averaged for each partial pressure of oxygen, measured on three separate days, and are shown in Figure 4 (top curve). A linear regression line reveals a rate constant for reaction A of $k = 9.2 \pm 0.5 \times 10^{-10}$ cm^3 s^{-1} (95% CL). This is in good agreement with the two previous reported values of this reaction of 8.5 $(-1, +4) \times 10^{-10}$ cm^3 s^{-1} by Johnsen and Biondi[26] and 8×10^{-10} cm^3 s^{-1} by Gieray et al.[27] Cornehl et al. measured this

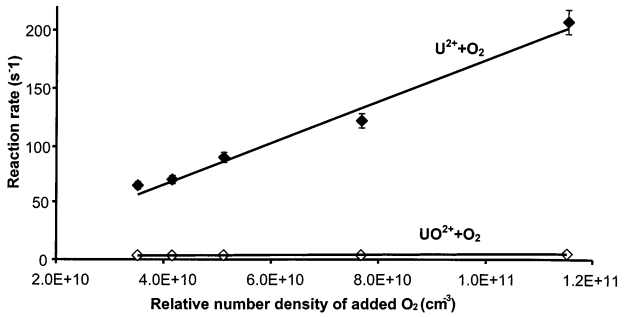

Figure 5. Measured reaction rates versus relative number density of added O_2 to determine the rate constants for the reactions of U^{2+} (filled diamonds) and UO^{2+} (open diamonds) with O_2. Values shown are the average of four different q_z values on three separate days with ±1 s.d.

rate as $1.17k_{ADO} \pm 40\%$,[31] and we interpret this to be $k = 6.5 \pm 2.6 \times 10^{-10}$ cm^3 s^{-1}, in reasonable agreement with the other values (to calculate k_{ADO},[32] the polarizability of O_2 was taken from reference 28).

3.2.2. UO^+ Reaction Rate with O_2. To observe reaction B, UO^+ ions were selectively isolated by applying a two-frequency resonance ejection on U^+ and UO_2^+, before allowing the reaction with admitted O_2 to proceed.

$$UO^+ + O_2 \rightarrow UO_2^+ + O^\bullet \qquad \text{(B)}$$

Measurements were again made at trapping potentials ranging from $0.2 \leq q_z \leq 0.8$, and no effect was found on the reaction rates. Figure 4 (lower curve) shows the averages of the rates measured at each O_2 pressure for four different trapping potentials. Data collected on three separate days are also included in the error bars (2σ, $n \sim 12$) in this plot to demonstrate the day-to-day repeatability of these experiments. The difference in the intercepts for the two lines shown in this figure is due to differences in the reactivity of U^+ and UO^+. It was found that U^+ readily reacts with residual water, while UO^+ reacts so slowly with water that the product is not observed prior to O_2 introduction.

The rate constant for reaction B is found to be $k = 9.0 \pm 0.6 \times 10^{-10}$ cm^3 s^{-1} (95% CL), the same as that of the bare uranium ion. Gieray et al. report a rate that corresponds to approximately 1×10^{-9} cm^3 s^{-1}, slightly faster than the reported rates for U^+. Their experiments were conducted in air, however, and this value assumes a 20% composition of O_2 in air and that no other species interfere with the measurement. Cornehl et al. report a rate of $0.95k_{ADO} \pm 40\%$,[31] and from this we calculate a k of $5.3 \pm 2 \times 10^{-10}$ cm^3 s^{-1}. No other rate constants for this reaction were found in the extant literature.

3.2.3. U^{2+} Reaction with O_2. The pulsed glow discharge ion source generates sufficient quantities of doubly charged ions that their reaction pathways and rates can also be examined. At these low pressures of oxygen it is possible to measure the very fast reaction C.

$$U^{2+} + O_2 \rightarrow UO^{2+} + O^\bullet \qquad \text{(C)}$$

Figure 5 (top curve) is a plot of the reaction rates of U^{2+} versus the relative added number density of oxygen. Analysis of the slope gives a rate constant of $1.8 \pm 0.4 \times 10^{-9}$ cm^3 s^{-1} (95% CL). Geiray et al. provide the only other known measurement of this rate as 1.3×10^{-9} cm^3 s^{-1}, again in reasonable agreement. It is interesting to note that although the predicted rate ($k_{ADO} = 1.1 \times 10^{-9}$ cm^3 s^{-1}) underestimates the measured rate constant for reaction C, the predicted rate for the doubly

charged uranium is twice the predicted rate of the singly charged uranium ion. The measured values for U^+ and U^{2+} (9.2 and 18 $\times$ 10^{-10} cm^3 s^{-1}, respectively) are at least consistent with predicted rates, viz., if both the reactions proceed at the collision rate then the rate for the doubly charged species should be twice that of the singly charged species.[32]

Because this reaction is exothermic, an upper limit of ΔH_f (UO^{2+}) $\leq$ 2028 kJ mol^{-1} can be obtained from reaction C, using values from Table 1. This limit is consistent with the value obtained by Cornehl et al. of ΔH_f (UO^{2+}) $\leq$ 2047 kJ mol^{-1}, obtained by the reaction of U^{2+} with CO_2.[33]

3.2.4. UO^{2+} Reaction with O_2. Reaction D is found to proceed with a pseudo-first-order rate constant of 3.7 $\pm$ 1 $\times$ 10^{-11} cm^3 s^{-1} (95% CL).

$$UO^{2+} + O_2 \rightarrow UO_2^{2+} + O^{\bullet} \qquad \text{(D)}$$

At any given pressure, reaction D is approximately 50 times slower than the bare uranium doubly charged ion and becomes rate limiting for the formation of UO_2^{2+} from U^{2+}. Cornehl et al. note that the rate of reaction D is more than 1 order of magnitude slower than reaction C, occurring at approximately 4% of the collision rate.[31,33] If we assume reaction C to occur at the collision rate, then reaction D occurs at approximately 2% of the collision frequency, in reasonable agreement with the previous reports.

3.2.5. UO_2^{2+} Reaction with O_2. Decreasing the low-mass cutoff value from 110 *m*/*z* to 25 *m*/*z* during the reaction period facilitated the observation of O_2^+, the charge exchange product of reaction E.

$$UO_2^{2+} + O_2 \rightarrow UO_2^{+} + O_2^{+} \qquad \text{(E)}$$

However, the reaction rate could not be measured satisfactorily because the reagent UO_2^{2+} could not be obtained in sufficient quantity. This is because reaction E proceeds at a rate faster than reaction D (>3.7 $\times$ 10^{-11} cm^3 s^{-1}) and prevents the accumulation of UO_2^{2+}. Resonant ejection of UO_2^{2+} during the reaction period of UO^{2+} with O_2 prevents the formation of both UO_2^+ and O_2^+, indicating that the alternative charge exchange reaction (not shown in Figure 1) in equation F is not an energetically feasible pathway.

$$UO^{2+} + O_2 \not\rightarrow UO^{+} + O_2^{+} \qquad \text{(F)}$$

This indicates that the ionization potential of UO^+ is less than that of O_2 (12.06 eV). Also, given that ΔH_f (O_2^+) = 1165 kJ mol^{-1} and ΔH_f (UO^+) = 582 $\pm$ 13 kJ mol^{-1}, the enthalpy of formation of UO^{2+} must be less than or equal to 1747 kJ mol^{-1}. This value is considerably smaller than the previous upper limits of 2028 kJ mol^{-1} obtained in section 3.2.3, and 2047 kJ mol^{-1} determined by Cornehl et al.[33]

3.3. Reactions with H_2O. The reactions that occur between uranium-containing ions and water are summarized in Figure 6. Isotopically enriched $H_2{}^{18}O$ was used in order to distinguish between the reactions with added $H_2{}^{18}O$ and those with residual $H_2{}^{16}O$ and $^{16}O_2$.

3.3.1. U^+ Reaction with H_2O. There seems to be some disagreement in the literature regarding the relative rates for reactions G and H.

$$U^+ + H_2O \rightarrow UO^+ + H_2 \qquad \text{(G)}$$

$$U^+ + H_2O \rightarrow UOH^+ + H \qquad \text{(H)}$$

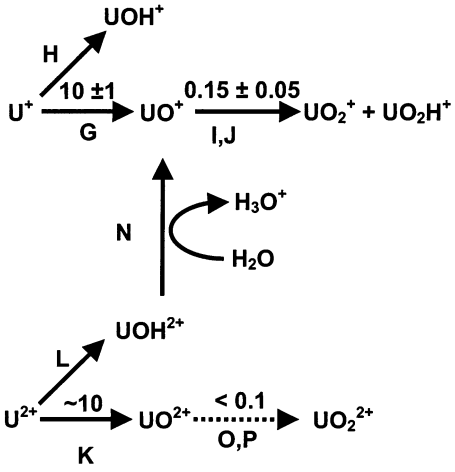

Figure 6. Reaction pathways for the reactions of U^{2+} and U^+ with gaseous H_2O. Rates shown have units of 10^{-10} cm^3 s^{-1}.

In low-energy ion beam experiments, both reactions were shown to be exothermic with a branching ratio of approximately 10:1 in favor of reaction G.[34] In ICR experiments, reaction H was not observed when the bare uranium ions were sufficiently cooled prior to the reaction.[31] The minor product UOH^+ was observed in the QIT with a branching ratio close to 10:1, in agreement with the ion beam experiments. From ion beam experiments, Armentrout and Beauchamp[34] propose a reaction mechanism in which the products of reactions G and H are formed from a similar reactive intermediate, $HU-OH^+$. They show that although both products are formed at the lowest kinetic energies explored, the formation of UO^+ is the thermodynamically favored product at low kinetic energies and that the UOH^+ product channel competes more at higher kinetic energies. The product ratio of ~10:1 observed in the QIT agrees with the lowest energy observations made by in the ion beam experiments by Armentrout and Beauchamp,[34] again indicating that the uranium ions are close to room temperature.

The total rate of loss of U^+ due to reaction with H_2O is 1.0 $\pm$ 1 $\times$ 10^{-9} cm^3 s^{-1}, slightly faster than the reaction with O_2 (reaction A). Armentrout and Beauchamp[34] also found the cross section for this reaction to be larger than the cross section for the reaction with O_2. Cornehl et al.[31] found the reaction rate constant with water to be $0.47k_{ADO}$ $\pm$ 40%, which equates to k = 8.1 $\times$ 10^{-10} cm^3 s^{-1}, also faster than the reaction rate with O_2. (This calculation was based on the polarizability and dipole values from ref 28 and a "locking factor" of 0.25 obtained from Su and Bowers.[32]) Sufficient quantities of UOH^+ could not be isolated in order to study the reactions between UOH^+ and H_2O.

3.3.2. UO^+ Reaction with H_2O. Reactions I and J have been shown to be exothermic processes.[34]

$$UO^+ + H_2O \rightarrow UO_2^{+} + H_2 \qquad \text{(I)}$$

$$UO^+ + H_2O \rightarrow UO_2H^{+} + H \qquad \text{(J)}$$

In the present work, the reaction between UO^+ and water was found to proceed at a rate of 1.5 $\pm$ 1 $\times$ 10^{-11} cm^3 s^{-1} and showed a branching ratio of approximately 1:1, in agreement with Armentrout and Beauchamp.[34] Cornehl and co-workers[31] state that the formation of UO_2H^+ was not observed in their studies. Experiments by Armentrout and Beauchamp and those presented here were conducted at much higher partial pressures (and total pressures) than the work of Cornehl et al. Higher

pressures would encourage three-body reactions, or subsequent cooling collisions by a third body, which would not be likely at lower pressures. In the absence of a third body it is possible that an initial exothermic step could provide the driving force to eliminate a molecule of H_2 from a reaction with water, i.e., reactions G and I. If a third body is present at a time frame shorter than that available for dehydrogenation, the third body could take away the excess energy and allow a lower energy channel (i.e., the loss of H) to be competitive, reactions H and J. In Armentrout and Beauchamp's experiments,[34] the third body would have to be another reagent molecule (because the collision cell pressure consists only of the reagent gas), but in these experiments the third body is more likely to be a neon bath gas atom.

3.3.3. U^{2+} Reaction with H_2O. Two possible reactions between U^{2+} and H_2O are given below

$$U^{2+} + H_2O \rightarrow UO^{2+} + H_2 \quad \text{(K)}$$

$$U^{2+} + H_2O \rightarrow UOH^{2+} + H \quad \text{(L)}$$

Although the charged products of reactions K and L differ in *m*/*z* by only 0.5, these ions can be selectively ejected from the QIT to determine the secondary reaction products of each ion. When UO^{2+} is resonantly ejected, the product mass spectra include the ions UOH^{2+}, H_3O^+, and UO^+ (as well as the starting reagent U^{2+}). No UOH^+ or H_2O^+ is observed, indicating that charge transfer between UOH^{2+} and H_2O (reaction M) does not occur.

$$UOH^{2+} + H_2O \not\rightarrow UOH^+ + H_2O^+ \quad \text{(M)}$$

Detection of the products UO^+ and H_3O^+ indicate that the reaction proceeds via the protonation of a water molecule in the reaction

$$UOH^{2+} + H_2O \rightarrow UO^+ + H_3O^+ \quad \text{(N)}$$

Thus, while it is not possible to form UO^+ from a reaction between U^{2+} and O_2, it is possible to form UO^+ from U^{2+} via the reaction with water, as demonstrated in the reaction sequence L and N. Because reaction L is exothermic, ΔH_f (H) = 218 kJ mol^{-1}, and ΔH_f (H_2O) = −241 kJ mol^{-1},[28] an upper limit of 1818 ± 50 kJ mol^{-1} is obtained for ΔH_f (UOH^{2+}). Likewise, given ΔH_f (H_3O^+) = 592 kJ mol^{-1} and that reaction N is also exothermic, a limit is also obtained for ΔH_f (UOH^{2+}) ≥ 1410 ± 13 kJ mol^{-1}. This bracketing gives limits for the enthalpy of formation of UOH^{2+} of 1410 ≤ ΔH_f (UOH^{2+}) ≤ 1818 kJ mol^{-1}.

Reliable reaction rate constants could not be determined for the doubly charged uranium ions because significant ion losses were observed during the course of the reactions. These losses could be due to an unidentified reaction loss path but are more likely due to scattering of the lighter ions that are formed during the reactions (i.e., $H_3{}^{18}O^+$). If all the U^{2+} losses do indeed pass quantitatively through UO^{2+} or UOH^{2+}, the reaction rate constant for the combined reactions K and L would be 1.0 × 10^{-9} cm^3 s^{-1}. This equates to approximately 0.4k_{ADO}. Because $H_3{}^{18}O^+$ was observed at low trapping potentials and the loss rate of UOH^{2+} was faster than the loss rate of UO^{2+}, the loss of charge is probably due to the fast protonation of water in the form of $H_3{}^{18}O^+$.

3.3.4. UO^{2+} Reaction with H_2O. Under the conditions of these experiments, reactions O and P were not observed.

$$UO^{2+} + H_2O \rightarrow UO_2{}^{2+} + H_2 \quad \text{(O)}$$

$$UO^{2+} + H_2O \rightarrow UO^+ + H_2O^+ \quad \text{(P)}$$

It is not established if these reactions are endothermic or just too slow to be measured. Because the slowest measurable rate on this system is approximately 1 × 10^{-11} cm^3 sec^{-1}, we provide this value as an upper limit for reactions O and P.

4. Conclusions

This work describes a methodology for measuring reaction rate constants in a quadrupole ion trap using neon as the bath gas. Kinetic energy effects are considered to be very small (contributing less than 5 kJ mol^{-1} to endothermic reactions) based on ion trap simulations and theoretical considerations. In the simulations, neon brings the kinetic energy of the ions to a steady state value more quickly than does helium, and this reduces the necessary cooling period before making a rate measurement. The reaction rates and products observed between uranium ions and $H_2{}^{18}O$ agree with work conducted in low energy ion beam experiments, but disagree, in select cases, with similar reactions observed in an ICR. These differences are likely to be the result of third body collisions in the QIT and ion beam experiments that help take away excess energy from the reaction intermediates.

The use of a neon bath gas is proving to be extremely useful for advanced applications of ion traps, including dissociating strongly bound oxide ions[19,20] and for measuring the thermodynamics and kinetics of reactions. It is hoped that these techniques will afford a promising approach to studying transuranic ions and compounds, where the QIT lends itself particularly well to radiation containment controls. Benefits would include size (for glovebox applications), cost, and the ability to measure reaction rates, thermochemistry, and bond dissociation energies (from CID rates) in a single instrument.

Acknowledgment. The authors thank John K. Gibson, of Oak Ridge National Lab, for many useful comments and suggestions during the preparation of this manuscript. We are also grateful to Graham Cooks for use of the ITSIM software. Research sponsored by the Division of Chemical Sciences, Geosciences, and Biosciences, Office of Basic Energy Sciences, U.S. Department of Energy, under contract DE-AC05-00OR22725 with Oak Ridge National Laboratory, managed and operated by UT-Battelle, LLC.

References and Notes

(1) Berkel, G. J. V.; Glish, G. L.; McLuckey, S. A. *Anal. Chem.* **1990**, *62*, 1284−1295.

(2) McLuckey, S. A.; Goeringer, D. E. *J. Mass Spectrom.* **1997**, *32*, 461−474.

(3) Vedel, F.; Vedel, M.; Brodbelt, J. S. Ion/Molecule Reactions. In *Practical Aspects of Ion Trap Mass Spectrometry*; March, R. E., Todd, J. F. J., Eds.; CRC Press: New York, 1995; Vol. 1, p 343.

(4) Bonner, R. F.; Lawson, G.; Todd, J. F. J. *Int. J. Mass Spectrom. Ion Phys.* **1972/73**, *10*, 197−203.

(5) Liere, P.; Steiner, V.; Jennings, K. R.; March, R. E.; Tabet, J. C. *Int. J. Mass Spectrom. Ion Processes* **1997**, *167/168*, 735−751.

(6) Armentrout, P. B.; Kickel, B. L. Gas-Phase Thermochemistry of Transition Metal Ligand Systems: Reassesment of Values and Periodic Trends. In *Organometallic Ion Chemistry*; Freiser, B. S., Ed.; Kluwer: Norwell, MA, 1996; Vol. 15.

(7) Lawson, G.; Bonner, R. F.; Mather, R. E.; Todd, J. F. J.; March, R. E. *J. Chem. Soc., Faraday Trans.* **1976**, *72*, 545−557.

(8) Fulford, J. E.; Dupuis, J. W.; March, R. E. *Can. J. Chem.* **1978**, *56*, 2324−2330.
(9) Dawson, P. H. *Int. J. Mass Spectrom. Ion Phys.* **1976**, *20*, 237−245.
(10) Armitage, M. A.; Higgins, M. J.; Lewars, E. G.; March, R. E. *J. Am. Chem. Soc.* **1980**, *102*, 5064−5068.
(11) Cutler, L. S.; Flory, C. A.; Giffard, R. P.; McGuire, M. D. *Appl. Phys. B* **1986**, *39*, 251−259.
(12) Schaaf, H.; Schmeling, U.; Werth, G. *Appl. Phys.* **1981**, *25*, 249−251.
(13) Siemers, I.; Blatt, R.; Sauter, T.; Neuhauser, W. *Phys. Rev. A* **1988**, *38*, 5121−5128.
(14) Vedel, F. *Int. J. Mass Spectrom. Ion Processes* **1991**, *106*, 33−61.
(15) Brodbelt-Lustig, J. S.; Cooks, R. G. *Talanta* **1989**, *36*, 255−260.
(16) Lovejoy, E. R.; Wilson, R. R. *J. Phys. Chem. A* **1998**, *102*, 2309−2315.
(17) Nourse, B. D.; Kenttamaa, H. I. *J. Phys. Chem.* **1990**, *94*, 5809−5812.
(18) Goeringer, D. E.; Duckworth, D. C.; McLuckey, S. A. *J. Phys. Chem. A* **2001**, *105*, 1882−1889.
(19) Duckworth, D. C.; Goeringer, D. E.; McLuckey, S. A. *J. Am. Soc. Mass Spectrom.* **2000**, *11*, 1072−1078.
(20) Jackson, G. P.; King, F. L.; Goeringer, D. E.; Duckworth, D. C. *Int. J. Mass Spectrom.* **2002**, *216*, 85−93.
(21) Goeringer, D. E.; Asano, K. G.; McLuckey, S. A. *Int. J. Mass Spectrom.* **1999**, *182/183*, 275−288.
(22) Duckworth, D. C.; Marcus, R. K. *J. Anal. At. Mass Spectrom.* **1992**, *7*, 711−715.
(23) Bui, H. A.; Cooks, R. G. *J. Mass Spectrom.* **1998**, *33*, 297−304.
(24) Viehland, L. A.; Mason, E. A. *J. Chem. Phys.* **1977**, *66*, 422−434.
(25) Wannier, G. H. *Bell Syst. Technol. J.* **1953**, *120*, 32.
(26) Johnsen, R.; Biondi, M. A. *J. Chem. Phys.* **1972**, *57*, 1975−1979.
(27) Gieray, R. A.; Reilly, P. T. A.; Yang, M.; Whitten, W. B.; Ramsey, J. M. *Anal. Chem.* **1998**, *70*, 117−120.
(28) *CRC Handbook of Chemistry and Physics*, 81st ed.; Lide, D. R., Ed.; CRC Press: New York, 2000.
(29) Lias, S. G.; Liebman, J. F.; Levin, R. D. *J. Phys. Chem. Ref. Data* **1984**, *13*, 695−808.
(30) Atkins, P. *Physical Chemistry*, 6th ed.; W. H. Freeman and Company: New York, 1998.
(31) Cornehl, H. H.; Wesendrup, R.; Diefenbach, M.; Schwarz, H. *Chem. Eur. J.* **1997**, *3*, 1083−1090.
(32) Su, T.; Bowers, M. T. *Int. J. Mass Spectrom. Ion Physics* **1973**, *12*, 347−356.
(33) Cornehl, H. H.; Heinemann, C.; Marcalo, J.; Pires de Matos, A.; Schwarz, H. *Angew. Chem., Int. Ed. Engl.* **1996**, *35*, 891−894.
(34) Armentrout, P. B.; Beauchamp, J. L. *Chem. Phys.* **1980**, *50*, 27−36.
(35) Hildenbrand, D. L.; Guvich, L. V.; Yungman, V. S. *The Chemical Thermodynamics of the Actinide Elements and Compounds Part 13.*; IAEA: Vienna, 1985.